Biochimica et Biophysica Acta 1833 (2013) 1904–1913

Contents lists available at SciVerse ScienceDirect

Biochimica et Biophysica Acta

journal homepage: www.elsevier.com/locate/bbamcr

PRIMA-1 induces autophagy in cancer cells carrying mutant or wild type p53

Debora Russo [a,1], Laura Ottaggio [b,1], Giorgia Foggetti [a,1], Matilde Masini [c], Pellegrino Masiello [c], Gilberto Fronza [a], Paola Menichini [a,*]

[a] U.O. Mutagenesi Molecolare e Riparazione del DNA, IRCCS Azienda Ospedaliera Universitaria San Martino-IST, 16132-Genova, Italy
[b] U.O. Anatomia e Citoistologia Patologica, IRCCS Azienda Ospedaliera Universitaria San Martino-IST, 16132-Genova, Italy
[c] Dipartimento di Patologia Sperimentale, Biotecnologie Mediche, Infettivologia ed Epidemiologia, Università di Pisa, Via Roma 55, Scuola Medica, 56126 Pisa, Italy

ARTICLE INFO

Article history:
Received 23 October 2012
Received in revised form 18 March 2013
Accepted 20 March 2013
Available online 29 March 2013

Keywords:
PRIMA-1
Autophagy
p53
LC3
Electron microscopy

ABSTRACT

PRIMA-1 is a chemical compound identified as a growth suppressor of tumor cells expressing mutant p53. We previously found that in the MDA-MB-231 cell line expressing high level of the mutant p53-R280K protein, PRIMA-1 induced p53 ubiquitination and degradation associated to cell death. In this study, we investigated the ability of PRIMA-1 to induce autophagy in cancer cells. In MDA-MB-231 and HCT116 cells, expressing mutant or wild type p53, respectively, autophagy occurred following exposure to PRIMA-1, as shown by acridine orange staining, anti-LC3 immunofluorescence and immunoblots, as well as by electron microscopy. Autophagy was triggered also in the derivative cell lines knocked-down for p53, although to a different extent than in the parental cells expressing mutant or wild type p53. In particular, while wild type p53 limited PRIMA-1 induced autophagy, mutant p53 conversely promoted autophagy, thus sustaining cell viability following PRIMA-1 treatment. Therefore, the autophagic potential of PRIMA-1, besides being cell context dependent, could be modulated in a different way by the presence of wild type or mutant p53. Furthermore, since both cell lines lacking p53 were more sensitive to the cytotoxic effect of PRIMA-1 than the parental ones, our findings suggest that a deregulated autophagy may favor cell death induced by this drug.

1. Introduction

In the last ten years a big effort has been employed in the identification and characterization of small molecules that target mutant p53 expressed in tumor cells [1]. One of these molecules, PRIMA-1 (for p53-reactivation and induction of massive apoptosis) has been identified as a compound that selectively inhibits the growth of tumor cells expressing mutant p53, by restoring the sequence-specific DNA-binding and transactivation functions of at least some mutant p53 proteins and promoting apoptosis [2]. It has been reported that into the cell, PRIMA-1 and its methylated form PRIMA-1^{Met} are converted to active products that form alkylated thiol groups in cysteine-containing proteins, including mutant p53; such a protein modification is considered sufficient to restore the tumor suppressor activity of p53 and induce apoptosis [3].

To date, a number of evidences support the notion that following p53 reactivation by PRIMA-1, different transcription-dependent and -independent pathways converging on apoptosis are indeed activated [4–6]. Interestingly, in human osteosarcoma Saos-2 cells PRIMA-1 has also been shown to induce several genes associated with the accumulation of unfolded proteins and endoplasmic reticulum (ER) stress such as XBP1, GRP78 and DNAJB2 [6–8]. Furthermore, a significant increase of the level of HSP70, a chaperone involved in protein folding, has been documented following PRIMA-1 treatment in different cell lines expressing mutant p53 [9,10]. In mutant p53 carrying cells, PRIMA-1 can also induce production of reactive oxygen species (ROS) [3], which in turn could trigger ER stress [11,12]. Conditions that disrupt ER function, including oxidative stress or accumulation of unfolded/misfolded proteins, may result in the unfolded protein response (UPR), a survival response acting to resolve deregulation of protein-folding pathways [13,14]. However, if the normal environment cannot be restored, the response to ER stress is switched from survival to apoptosis. Interestingly, accumulating evidence suggests that the ER may play an important role not only in apoptosis but also in the regulation of autophagy [15].

Autophagy is a dynamic catabolic process in which cellular proteins, organelles, and cytoplasmic constituents are degraded and recycled to sustain cell metabolism [16,17]. At the first step of autophagy, a double membrane engulfs cytoplasmic components and forms vesicles called "autophagosomes". Afterwards, the fusion of autophagosomes with lysosomes results in the formation of autophagolysosomes, where the sequestered contents are degraded and recycled for protein and ATP synthesis [18,19]. The role of autophagy in modulating tumor growth is undoubtedly complex. At the stage of tumor development, autophagy

* Corresponding author at: Molecular Mutagenesis and DNA Repair Unit, IRCCS AOU San Martino-IST, L.go R. Benzi, 10, Genova, Italy. Tel.: +39 010 555 8225; fax: +39 010 555 8237.
E-mail address: paola.menichini@istge.it (P. Menichini).
[1] These authors equally contributed to the work.

0167-4889/$ – see front matter
http://dx.doi.org/10.1016/j.bbamcr.2013.03.020

may function as a tumor suppressor mechanism, as suggested by the observation that deletions of autophagic genes such as *UVRAG* and *beclin1* are frequently found in human cancers [20–22]. On the other side, the activation of autophagy often occurring in the poorly vascularized central areas of a solid tumor may function as a survival mechanism against hypoxia and nutrient deprivation. In this case, autophagy may contribute to tumor progression by enhancing oncogenic functions [22,23].

It is known that the regulation of autophagy depends on an intricate network of proteins among which p53, a key component of the cellular response to different types of stress [24], may play a dual role [25]. In fact, whereas wild type p53 may inhibit autophagy when localized in the cytoplasm [26], after its transfer into the nucleus it can transactivate pro-autophagic genes such as DRAM [27]. However, it has been shown that deletion of wild type p53 can favor autophagy induction in human and mouse cells, indicating that p53 may act as an endogenous repressor of the autophagic process [26].

We have previously found that in the MDA-MB-231 cell line deriving from a human breast carcinoma and expressing high level of the mutant p53-R280K protein, PRIMA-1 induced a significant nucleolar redistribution of mutant p53, associated to p53 degradation *via* ubiquitination, and cell death. Our results suggested that in some cellular context, PRIMA-1 cytotoxicity could be at least partially due to the triggering of a protein degradation pathway that removes a pro-survival function of the mutant p53 itself [10].

On the basis of these evidences, and to get insights into the involvement of p53 in the autophagic process, in this study we investigate the ability of PRIMA-1 to induce autophagy in cancer cells carrying mutant or wild type p53 protein, such as MDA-MB-231 and HCT116 cells, respectively, and in their derivative cell lines knocked-down for p53.

2. Materials and methods

2.1. Cell culture and drug treatment

MDA-MB-231 cell line (human breast carcinoma) carrying the p53-R280K mutation [28], as confirmed by us (not shown), was authenticated by DNA (STR) profiling (DSMZ, Braunschweig, Germany). The mutant p53 knocked-down T1 cell line was obtained as described [10]. HCT116 wt p53 +/+ and HCT116 wt p53 −/− cells were obtained by Dr. B. Vogelstein (The Johns Hopkins Kimmel Cancer Center, Baltimore, MD). MCF7 (wild type p53), DLD1 (mutant p53-S241F) and normal MRC5 (wild type p53) cells were obtained by the Interlab Cell Line Collection (ICLC Genova, Italy). Cells were grown in D-MEM (MDA-MB-231, T1, MCF7), RPMI (HCT116, DLD1) and MEM (GIBCO Invitrogen, Milano, Italy) containing 5% (MDA-MB-231, T1) and 10% (DLD1, HCT116, MRC5) foetal bovine serum (Euroclone, Milano, Italy), and maintained at 37 °C in 5% CO_2 at 100% humidity. PRIMA-1 (Calbiochem-Merck, Milan, Italy) was dissolved in H_2O at a concentration of 10 mM and working solutions were then prepared by appropriate dilutions in PBS. Rapamycin (Sigma-Aldrich, Milano, Italy) was dissolved in DMSO at a concentration of 2.74 mM. Starvation medium was obtained by adding 0.25 % serum to D-MEM and 0.5% serum to RPMI for MDA-MB-231/T1 and HCT116 cells, respectively.

2.2. Detection of acidic vesicular organelles (AVOs)

At 24 h after treatment, cells were incubated with medium containing 1 μg/ml acridine orange (Sigma-Aldrich, Milano, Italy) for 15 min at room temperature. The acridine orange was then removed, and unfixed cells were rapidly washed in fresh medium and immediately examined by fluorescence microscopy. Micrographs were taken using an epifluorescence Provis AX70 microscope (Olympus, Tokyo, Japan) and Cytovision software (Applied Imaging Corp., Santa Clara, CA, USA). Autophagy occurrence was based on the presence of cells displaying intense red staining in response to a given experimental treatment.

2.3. Immunocytochemistry and LC3 detection

Cells were seeded on coverslips and treated for 24 h. At the end of treatments, slides were washed twice with PBS, fixed in 1:1 methanol:acetone and incubated with anti MAPLC3 antibody (Sigma-Aldrich, Milano, Italy) for 1 h at 37 °C, followed by an anti-rabbit FITC-conjugated antibody (Sigma-Aldrich, Milano, Italy). Slides were then counterstained by 4,6-diamidino-2-phenylindole (DAPI). Amount of cells containing LC3-puncta was determined by scoring at least 100 cells and documented as described above.

2.4. Western blot analysis

Standard cell extracts were prepared as described [29]. Anti MAPLC3 (L8918, Sigma-Aldrich, Milano, Italy) and anti β-actin (AC-74, Sigma-Aldrich, Milano, Italy) antibodies were employed. Secondary anti-mouse IgG peroxidase conjugate (A9044) and secondary anti-rabbit peroxidase conjugate (A9169) were from Sigma-Aldrich. Detection was carried out with ECL-Plus Western Blotting Detection System (Amersham, Milano, Italy).

2.5. Electron microscopy analysis

Cultured cells were fixed in 2.5% glutaraldehyde in 0.1 M phosphate buffer (pH 7.3) for 20 min at room temperature, washed in 0.1 M phosphate buffer (pH 7.4), post-fixed in 0.1% osmium tetroxide in 0.1 phosphate buffer (pH 7.4) and dehydrated in a graded series of ethanol. During the last de-hydration phase, the cells were scraped and centrifuged to obtain a pellet that was briefly transferred to propylene oxide and embedded in PolyBed 812 (Polyscience Inc., Warrington, Pa, USA). Ultrathin sections were cut with a diamond knife, stained with uranyl acetate and lead citrate and observed under a Zeiss 902 transmission electron microscope [30]. Autophagic vacuoles (AV) were identified as double-membraned vesicles containing degenerating cytoplasmatic organelles or cytosol, while residual bodies (RB) were identified as single-membraned electron dense bodies containing unidentifiable material [16,31]. Morphometric analyses were performed by stereological techniques [32]. In particular, the volume density of AV and RB was estimated. Ten microphotographs of each experimental condition were taken, at an original magnification of ×3000. Volume density values derived from the evaluation of 15–20 different cells for each cell category (in most micrographs there were more than one cell). The cytoplasm was used as reference area. A graticule (11 × 11) composed of 169 points was placed on the micrographs and the number of points intersecting the AVs was counted. Volume density of AV was calculated according to the formula: volume density = Pi/Pt, where Pi is the number of points within the subcellular component and Pt is the total number of points, and expressed in ml/100 ml of tissue (ml%) [32]. The number of AV and RB per area unit was calculated as the mean of the number of these subcellular components contained in a photographic area corresponding to a real area of 220 μm^2 [33].

2.6. Real-time monitoring of cell proliferation

The xCELLigence Real-Time Cell Analyzer (RTCA) Instrument® (Roche) monitors cell proliferation in real time by measuring electrical impedance across micro-electrodes integrated on the bottom of special tissue culture plates (E-plates). Cell spreading and proliferation are expressed as an arbitrary unit called Cell Index (CI), which is the result of the number of cells, cell morphology and cellular adhesion to the plates [34]. For cell proliferation assays, 50 μl of media was added to the E-plate to obtain background readings, followed by the addition of

50 μl of cell suspension at different densities depending on cell type. The E-plates containing the cells were incubated at room temperature for 30 min and placed on the reader in the incubator. Impedance-based CI was measured with time intervals varying from 5 to 30 min. After 24 h the cells were treated with different concentrations of PRIMA-1 and monitored every 30 min for the designed period of time.

3. Results

3.1. PRIMA-1 induces autophagy in cancer cells carrying mutant p53

To determine whether PRIMA-1 can induce autophagy we used different approaches. First, we used an assay that measures supravital staining of acidic compartments. Indeed, in the late phase of autophagy, the autophagolysosome generates an acidic compartment which can be stained with acridine orange (bright red or orange fluorescence) [35,36]. An increase in acridine orange-positive acidic vesicular organelles (AVOs) occurs in conjunction with the induction of autophagy [37,38]. In MDA-MB-231 cells the presence of red AVOs following PRIMA-1 treatment (200 μM), as well as serum-deprivation or rapamycin, two well-known stimuli used as positive controls of autophagy induction, was detected (Fig. 1A). In contrast, mock-treated cells exhibited minimal red fluorescence. Interestingly, the induction of AVOs by PRIMA-1 appears at least as strong as that determined by rapamycin and stronger than after starvation, suggesting that PRIMA-1 is quite efficient in triggering the autophagic response.

The microtubule-associated protein 1 light chain 3 (LC3) was used as further marker of autophagy. When autophagy is not activated, LC3 is localized homogeneously in the cytoplasm, while upon initiation of autophagy, it associates with the membrane of autophagosomes. An antibody against endogenous LC3 protein was used to detect autophagy by immunofluorescence. As shown in Fig. 1C, in MDA-MB-231 cells, a variable number of large LC3 puncta of intense green cytoplasmic fluorescence, likely representing LC3 bound to AVs, appeared after exposure of cells to starvation, rapamycin and PRIMA-1. While mock cells were negative for green LC3 puncta, a small number of positive cells were observed after serum starvation, whereas a marked increase of cells containing LC3 puncta was detected after 200 μM PRIMA-1 treatment (Fig 1C, D). The presence and modulation of activated 16-kDa LC3-II isoform, derived from the autophagy-related proteolytic conversion of the 18-kDa precursor LC3-I [39], was also checked by western blot (Fig 1B). The level of LC3-II was already high in untreated cells and did not increase after PRIMA-1 treatment. Indeed, high level of endogenous LC3-II under nutrient-rich conditions has been already observed in MDA-MB-231 cells [31,40] indicating that, in this cell line, the level of LC3-II determined by western blot may not be a suitable marker for autophagic activity.

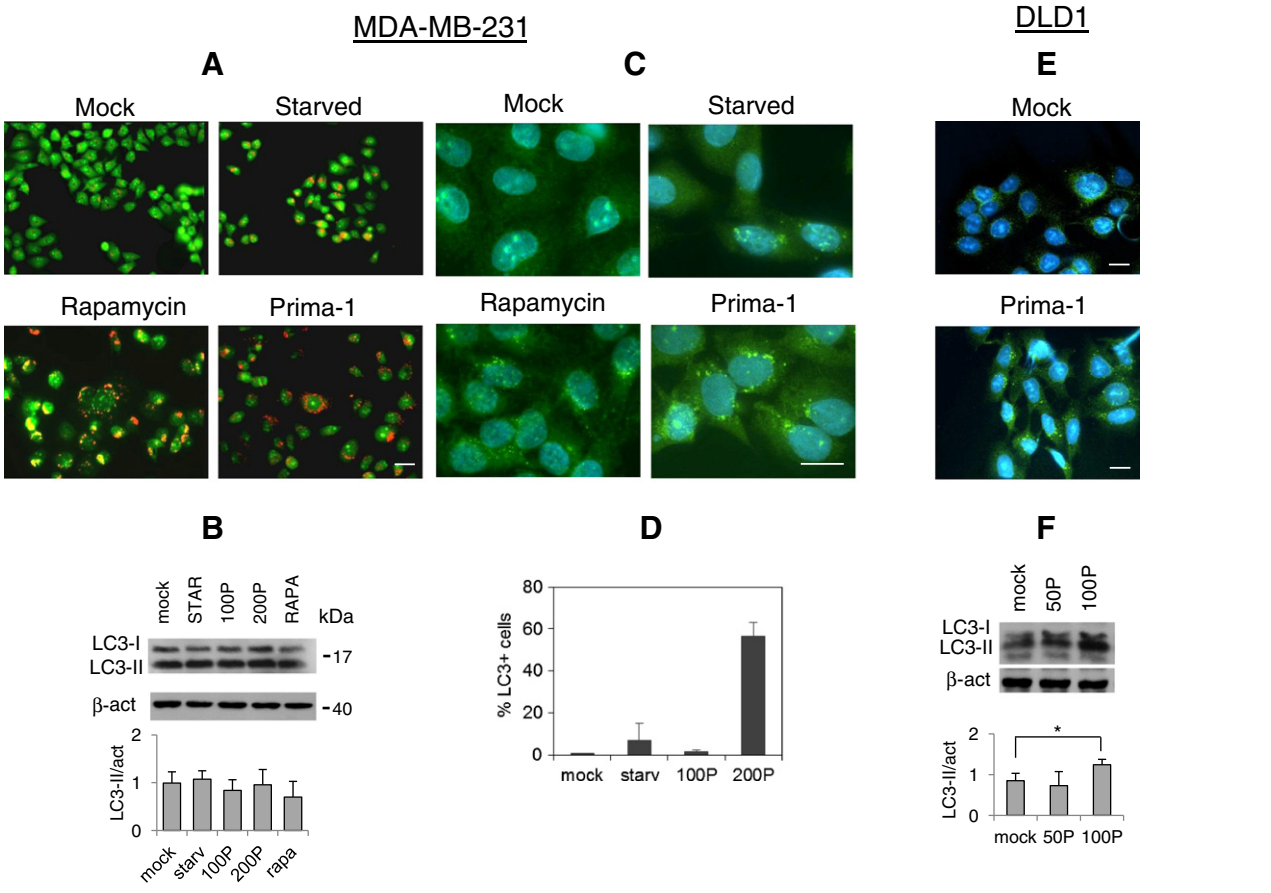

Fig. 1. Induction of autophagy in MDA-MB-231 and DLD1 cells. A) MDA-MB-231 cells were serum-starved or treated with either rapamycin (100 nM) or PRIMA-1 (200 μM). Supravital cell staining with acridine orange was performed after 24 h of treatment. In mock cells, the cytoplasm and nucleus revealed a green fluorescence, while in serum-starved, rapamycin and PRIMA-1 treated cells, bright red acidic vescicular organelles (AVOs) were observed. Bar 10 μm. B) Representative western blots showing LC3-I and LC3-II bands detected with the anti-LC3 antibody in serum-starved, rapamycin and PRIMA-1-treated cell lysates. The histogram was obtained after densitometric scanning of the images from 3 to 5 independent experiments; the amount of LC3-II form was normalized for β-actin. C) MDA-MB-231 cells were treated as above and fixed for immunostaining with an antibody against endogenous LC3. Representative images from two independent experiments are shown. D) The percentage of LC3 puncta-containing cells is reported in the histogram. E) DLD1 cells were mock-treated or treated for 24 h with 50 μM PRIMA-1 and fixed for immunostaining with an antibody against endogenous LC3. F) Representative western blots showing LC3-I and LC3-II bands in PRIMA-1-treated DLD1 cell lysates. The histogram was obtained after densitometric scanning of the images from at least three independent experiments; the amount of LC3-II form was normalized for β-actin and expressed as fold increase *vs* the mock-treated DLD1 samples. The increase of LC3-II form in 100 μM PRIMA-1 compared to mock-treated cells was statistically significant (*$p = 0.03$ paired *t*-test).

The induction of autophagy was also investigated in DLD1, a colon cancer cell line carrying the mutant p53S241F. In these cells, both the appearance of LC3 positive vacuoles in immunofluorescence experiments (Fig. 1E) and the increase of LC3-II band in western blot (Fig. 1F) were detected after exposure to PRIMA-1. This indicates that the induction of autophagy by PRIMA-1, detected in DLD1 at lower drug concentrations than in MDA-MB-231 cells, was not cell-type specific. Even though the 200 μM PRIMA-1 concentration used in MDA-MB-231 cells might appear high, in a first-in-human study with PRIMA-1^{Met} (APR-246) the maximum tolerated dose, 60 mg/kg, correlates to a maximum plasma concentration of about 300 μM [41]. Thus, the concentrations used in our *in vitro* experiments are compatible with the doses used in those patients.

Electron microscope (EM) analysis was performed in MDA-MB-231 cells. In the cytoplasm, mitochondria appeared often swelled with disrupted cristae and dispersed matrix. Furthermore, markedly dilated and fragmented ER cisternae (a clear index of ER stress) were observed (Fig. 2A). The morphometric analysis of EM images confirmed that the volume density of ER in PRIMA-1 treated and starved MDA-MB-231 cells significantly ($p < 0.05$, at least) increased as compared to mock cells [ER volume density (ml%): mock 0.2 ± 0.03, PRIMA-100 μM 2.1 ± 0.15, starvation 0.6 ± 0.08]. Several double-membraned autophagosomes or AVs were detected after starvation, rapamycin and or PRIMA-1 treatment (Fig. 2A). At 200 μM PRIMA-1, AVs were large and numerous, sometimes filling wide cytoplasmic areas. In general, AVs contained membrane residues or fragmented mitochondria, these latter being more often present upon PRIMA-1 treatment. Interestingly, besides classical AVs, numerous electron dense single membrane-limited autophagolysosomes or residual bodies (RB) were identified (Fig. 2A, lower right panel). These RBs, containing unrecognizable material or cell debris, are believed to be the remnants of the auto-degradative activity occurring after fusion of lysosomes with AVs, thus representing the late steps of the autophagic process [31]. The morphometric analysis revealed a significant increase with respect to control cells ($p < 0.05$) of the number and volume density of AVs after PRIMA-1 treatment in a dose-dependent fashion, as well as after serum starvation (Fig. 2B). On the other hand, the number and volume density of RBs significantly increases following 200 μM PRIMA-1 treatment but not following starvation (Fig. 2B).

Altogether, these results indicate that PRIMA-1 is able to induce an autophagic process in cancer cells carrying mutant p53.

3.2. PRIMA-1 induces autophagy in MDA-MB-231 cancer cells knocked-down for mutant p53

Since p53 may have a regulatory role in autophagy [26,27], we investigated whether the presence of mutant p53 affects the autophagic potential of PRIMA-1. To this aim, the LC3 localization was determined in T1, a MDA-MB-231 derivative cell line in which the mutant p53 has been knocked down by RNA interference [10]. In the absence of treatment, approximately 20% of T1 cells could be classified as carrying LC3 puncta by immunofluorescence analysis. A three-fold increase of LC3 puncta containing cells was observed only upon 200 μM PRIMA-1 treatment (Fig 3A).

As in MDA-MB-231, in T1 cells the EM analysis revealed the presence of swelled and disrupted mitochondria with dispersed matrix. The occurrence of ER stress was also documented; indeed, the volume density of ER in PRIMA-treated and starved T1 cells significantly ($p < 0.05$, at least) increased as compared to mock cells [ER volume density (ml%): mock 0.3 ± 0.05, PRIMA-100 μM 1.9 ± 0.16, starvation 2.6 ± 0.16]. A significant increase in AV number and volume density in both starved and 200 μM PRIMA-1 treated cells was detected (Fig. 3B, C). On the other hand, the RB number and volume density increased following 100 μM PRIMA-1 while after serum starvation was significantly lower than in untreated cells (Fig 3C).

When a comparison between the morphometric data of MDA-MB-231 and T1 cells was considered, we found that following treatment with 200 μM PRIMA-1 the number of AVs, as well as their volume density, was significantly lower in T1 than in MDA-MB-231 (AV n: 4.2 ± 0.2 *vs* 7.5 ± 0.2, $p < 0.05$; AV vol density: 2.7 ± 0.21 *vs* 3.9 ± 0.1, $p < 0.05$). Following starvation, there was no difference in the number of AVs between T1 and MDA-MB-231 (AV n: 2.8 ± 0.1 *vs* 3.2 ± 0.5), although their volume seems to increase more in MDA-MB-231 than in T1 cells. When the level of basal autophagy

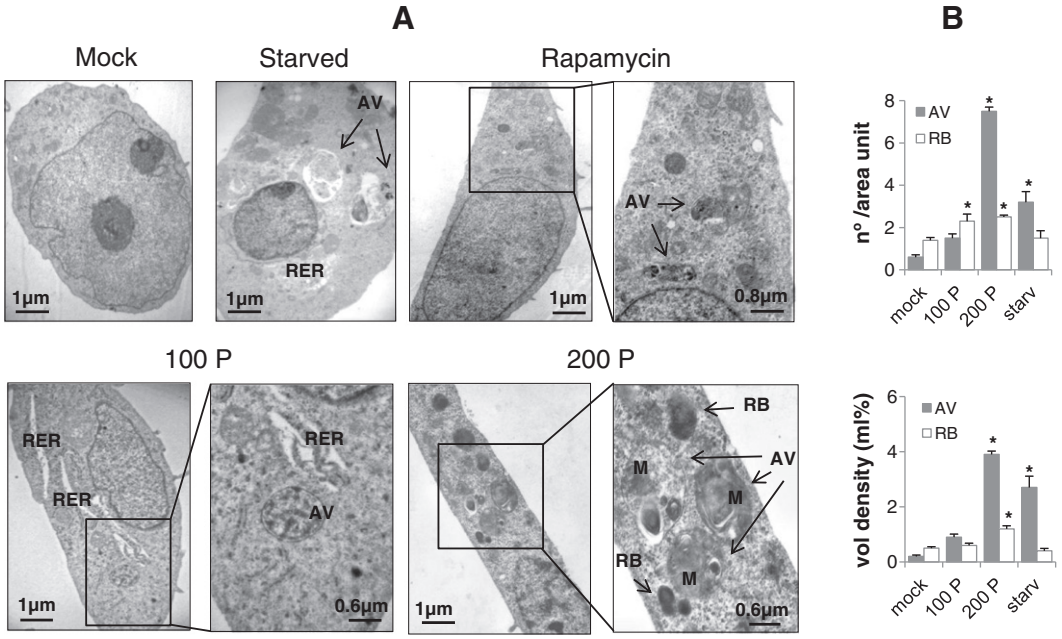

Fig. 2. Autophagy detection by EM in MDA-MB-231 cells. A) Representative EM images of MDA-MB-231 cells treated as in Fig. 1. Accumulation of AVs can be observed after treatment with rapamycin, starvation, 100 μM PRIMA-1 (100P) and 200 μM PRIMA-1 (200P). AVs, sometimes containing mitochondria (M), and RBs are indicated by arrows; RER = rough endoplasmic reticulum. Up to 200 cells were scored. B) Histograms show the morphometric analysis of the number and volume density of AVs and RBs in MDA-MB-231 cells exposed to serum starvation and PRIMA-1 (100 μM and 200 μM). Bars indicate standard error; *$p < 0.05$, at least, *vs* mock-treated cells.

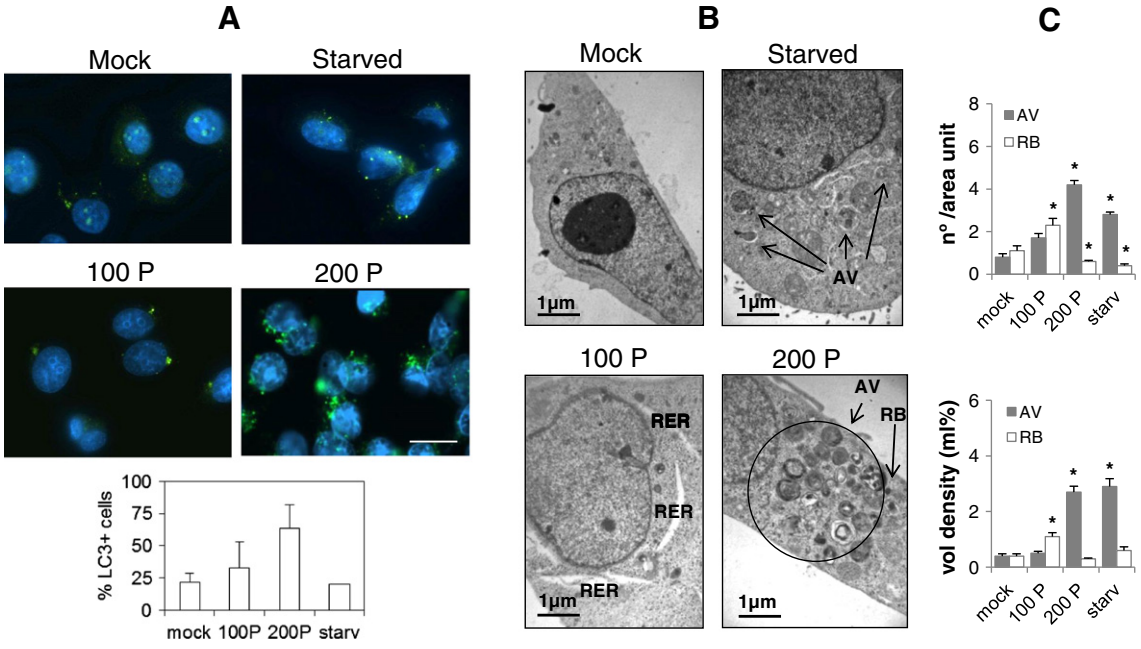

Fig. 3. Induction of autophagy in T1 cells. A) T1 cells were serum-starved or treated with 100 μM or 200 μM PRIMA-1 for 24 h and fixed for immunostaining with an anti-LC3 antibody. Representative images of endogenous LC3 from two independent experiments are shown. Bar 10 μm. In the lower panel, the percentage of LC3 puncta-containing cells is reported. B) Representative micrographs of T1 cells treated as above. AVs and RBs can be observed occasionally in mock-treated cells and much more after starvation or incubation with PRIMA-1. RER = rough endoplasmic reticulum. Up to 200 cells were scored. C) Histograms show the morphometric analysis of the number and the volume density of AVs and RBs in T1 cells exposed to serum starvation and PRIMA-1. Bars indicate standard error; *$p < 0.05$, at least, *vs* mock-treated cells.

was taken into consideration, also immunofluorescence analysis evidenced a lower induction of autophagy in T1 than in MDA-MB-231 cells (compare Figs. 1C,D and 3A). These observations suggest that the presence of mutant p53 may potentiate the autophagic response to 200 μM PRIMA-1.

Thus, PRIMA-1 induced autophagy also in T1 cells lacking mutant p53. However, the removal of mutant p53 resulted in increased levels of basal autophagy but in reduced PRIMA-1-induced autophagy.

3.3. PRIMA-1 induces autophagy in wild type p53 carrying cancer cells

We then investigated the ability of PRIMA-1 to induce autophagy in HCT116 cancer cells carrying or lacking wild type p53. The real time monitoring of cell proliferation (Fig 4) (see Materials and methods for description) showed a higher sensitivity of the HCT116 p53 −/− cells to the cytotoxic effect of PRIMA-1 than their p53 +/+ counterpart.

Treatment with PRIMA-1 determined a clear-cut increase in distinct LC3 puncta in both cell lines (Fig. 5A). In HCT116 p53 +/+, at 50 and 100 μM PRIMA-1, an increasing number of cells showed large fluorescent agglomerates not present in untreated control cells (Fig. 5A). Conversely, a relevant percentage of control HCT116 p53 −/− cells (45%) showed tiny spots and upon treatment with 50 μM PRIMA-1, the number and brightness of these spots were enhanced and the percentage of cells containing them increased up to 75%. The toxicity of the 100 μM PRIMA-1 dose in these cells did not allow the evaluation by such technique. Western blot analysis was performed with anti-LC3 antibody (Fig. 5B). A significant increase in activated 16-kDa LC3-II isoform was found in both cell lines exposed to 100 μM PRIMA-1 as compared to mock-treated cells ($p < 0.005$ in 100 μM PRIMA-1 *vs* mock in HCT116 p53 +/+; $p = 0.007$ in 100 μM PRIMA-1 *vs* mock in HCT116 p53 −/−). Furthermore, a higher level of LC3-II in both mock and 100 μM PRIMA-1 treated HCT116 p53 −/− cells compared to HCT116 p53 +/+ cells was found ($p < 0.05$).

The EM analysis revealed the induction of numerous AVs in both HCT116 cell lines upon PRIMA-1 treatment as well as following starvation (Fig. 6). In HCT116 p53 −/− treated cells, AVs were larger and more abundant than in p53 +/+ treated cells. At both PRIMA-1 doses in p53 −/− cells and at the higher dose in p53 +/+ cells, AVs containing still recognizable mitochondria could be observed at higher magnification in many cells (not shown). The number and volume density of AVs significantly increased in both cell lines after PRIMA-1 treatment and serum starvation. Noteworthy, HCT116 p53 −/− cells presented the highest AV number when exposed to 50 μM PRIMA-1 (Fig. 6B). Also in HCT116 cells, as previously observed in MDA-MB-231

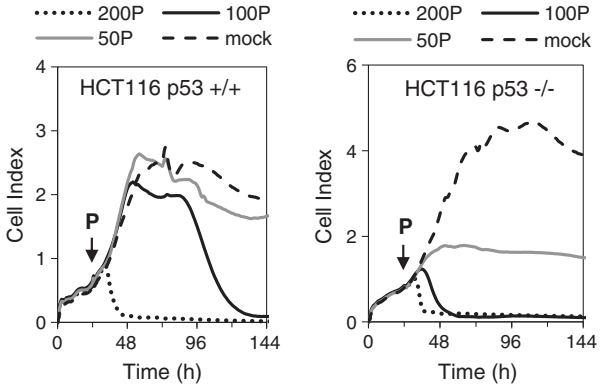

Fig. 4. Real-time monitoring of cell proliferation following PRIMA-1 treatment. HCT116 p53 +/+ and HCT116 p53 −/− cells were plated in suitable E-plates and their cell index was monitored continuously. Due to their different morphologies (with HCT116 p53 −/− cells larger than HCT116 p53 +/+ cells), the untreated HCT116 p53 −/− cells reached a plateau at a higher cell index than the HCT116 p53 +/+ cells after approximately the same time interval. Twenty-four hours after plating, different concentrations of PRIMA-1 (P) were added and cell growth was monitored every 30 min up to 144 h. The growth of HCT116 p53 +/+ cells was not affected until 36 h after the addition of 100 μM PRIMA-1. On the other hand, the HCT116 p53 −/− cells stop to proliferate and level off when exposed to 50 μM PRIMA-1 while they detach from the plate approximately 12 h after the addition of 100 μM PRIMA-1. The 200 μM PRIMA-1 concentration was very toxic for both cell lines.

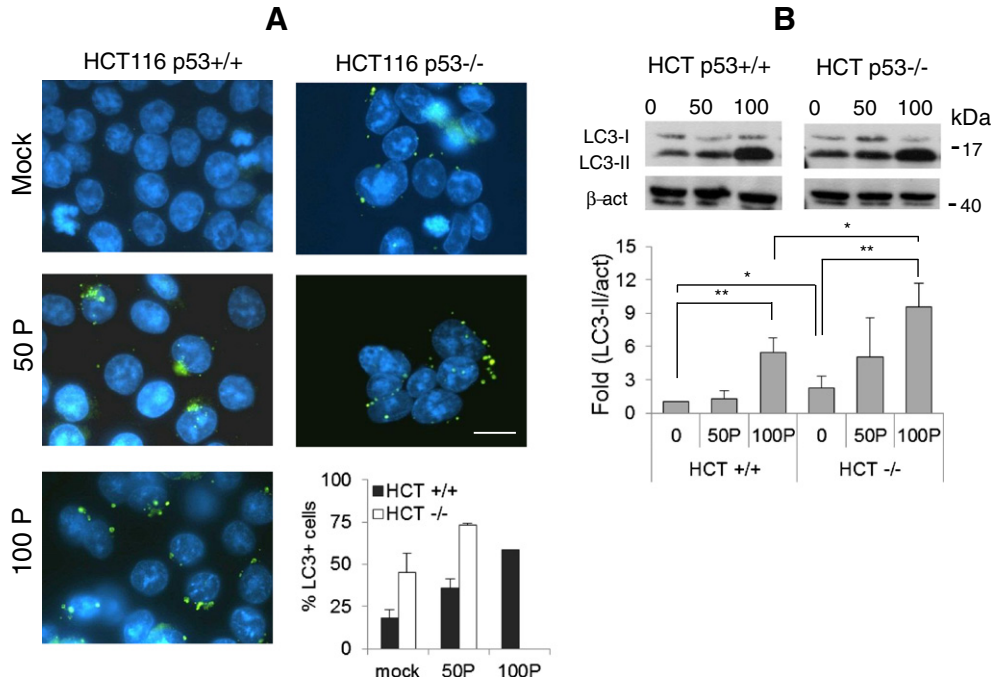

Fig. 5. PRIMA-1-induced autophagy in HCT116 cells. A) Representative images of immunofluorescence analysis of endogenous LC3 localization in PRIMA-1 treated (50 μM and 100 μM) HCT116 p53 +/+ and HCT116 p53 −/− cells. Due to their high PRIMA-1 sensitivity, HCT116 p53 −/− cells could not be retrieved after exposure to 100 μM PRIMA-1, making the immunofluorescence analysis of this experimental point not feasible. Bar 10 μm. In the lower right panel, the percentage of LC3 puncta-containing cells is reported. B) Representative western blots showing LC3-I and LC3-II bands in PRIMA-1-treated cell lysates, detected with the antibody against endogenous LC3. The histogram was obtained after densitometric scanning of the images from at least three independent experiments; the amount of LC3-II form was normalized for β-actin and expressed as fold increase *vs* the untreated HCT116 p53 +/+ samples. The fold increase of LC3-II form in 100 μM PRIMA-1 compared to untreated cells was statistically significant in both cell lines (**$p < 0.005$ for HCT116 p53 +/+; **$p = 0.007$ for HCT116 p53 −/−) as well as the difference between the amount of LC3-II in HCT116 p53 −/− *vs* HCT116 p53 +/+ in mock and 100 μM PRIMA-1 treated cells (unpaired *t*-test, *$p < 0.05$).

and T1 cells, the number and volume density of RBs increased more upon treatment with PRIMA-1 than upon starvation.

The comparison between the morphometric data obtained in HCT116 p53 +/+ and HCT116 p53 −/− cells revealed a more efficient induction of autophagy in HCT116 p53 −/− than in p53 +/+ cells following 50 μM PRIMA-1 (AV n: 6.6 ± 0.6 *vs* 1.8 ± 0.3. $p < 0.05$; AV vol: 2.6 ± 0.2 *vs* 0.7 ± 0.1, $p < 0.05$). Furthermore, as determined by immunofluorescence, the percentage of cells containing LC3 puncta

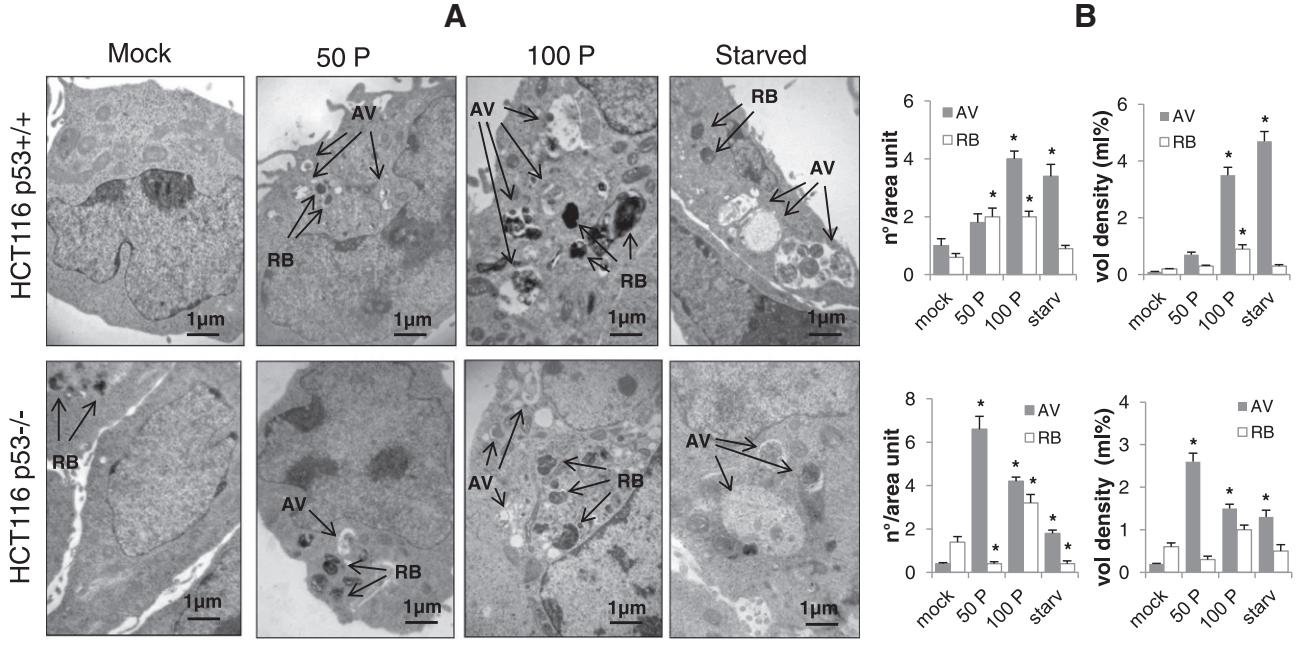

Fig. 6. EM analysis of HCT116 p53 +/+ and HCT116 p53 −/− cells after PRIMA-1 treatment and serum starvation. A) In HCT116 p53 −/− cells autophagy could be detected in some mock cells and in numerous PRIMA-1 treated cells. An engulfment of AVs and RBs could be observed in HCT116 p53 +/+ and HCT116 p53 −/− cells after incubation with 100 μM PRIMA-1. B) Histograms show the morphometric analysis of the number and the volume density of AVs and RBs in HCT116 cells exposed to serum starvation and PRIMA-1. *$p < 0.05$ at least *vs* mock-treated cells.

was higher in the untreated HCT116 p53 −/− than in untreated HCT116 p53 +/+ cells.

In addition to HCT116 cells, autophagy was also investigated in the MCF7 breast cancer cells and in normal, not tumor-derived MRC5 cells carrying wild type p53. In MCF7, the appearance of LC3 positive cells in immunofluorescence assays, as well as the increase of the LC3-II band in western blot showed an autophagic response triggered by PRIMA-1 (see Supplementary Fig. 2). In MRC5, we could observe an increase of LC3-II band following 75 μM PRIMA-1 (Supplementary Fig. 2) suggesting the occurrence of autophagy also in normal cells.

Thus, PRIMA-1 induces autophagy in cancer cells carrying wild type p53. However, in cells lacking wild type p53, as HCT116 p53 −/− cells, both a higher basal level of autophagy and a stronger induction of autophagic markers following PRIMA-1 could be observed.

4. Discussion

The results of this study provide clear evidence that PRIMA-1, a low-molecular-weight synthetic compound known to exert selective growth inhibition of tumor cells expressing mutant p53, induces autophagy in cancer cells carrying both mutant and wild type p53. Autophagy occurrence was detected by acridine orange staining, anti-LC3 immunofluorescent puncta and immunoblots, as well as by EM observation of double-membraned AVs. Very interestingly, ultrastructural analysis revealed significant alteration of the ER. The ability of PRIMA-1 to affect ER homeostasis has been previously suggested on the basis of the observation that in Saos-2 cells carrying mutant p53, PRIMA-1^{Met} induced several genes associated with ER stress [6]. However, our results represent the first direct evidence that ER is indeed a target of PRIMA-1 action. It is also noteworthy that ER stress has been recognized as a putative regulator of the autophagic signaling pathways, mainly but not exclusively through the activity of BCL-2 family proteins [15,42], which supports the idea that a link between PRIMA-1-induced ER stress and autophagy actually exists. Mitochondrial damage can be also induced by PRIMA-1 as documented by the presence of apparently well preserved or fragmented mitochondria in the AVs. This might originate from a massive induction of signaling cascades that target mitochondria as demonstrated in cancer cells carrying exogenous mutant p53 treated with PRIMA-1^{Met} [5].

The autophagy induced by PRIMA-1 appeared different from that induced by serum starvation, a stimulus known to trigger a typical autophagic process with a pro-survival function. Enhanced immunofluorescence detection of LC3 puncta and the presence of numerous AVs were a more frequent feature of PRIMA-1-treated cells than serum-starved cells. Interestingly, abundant acridine orange-positive AVOs as well as several RBs at ultrastructural level were identified following PRIMA-1, but not after starvation. Such RBs containing unrecognizable material or cell debris, are believed to be the remnants of the auto-degradative activity occurring after fusion of lysosomes with autophagocytic vacuoles, thus representing the late steps of the autophagic process [31]. As such, they could probably be viewed as the ultrastructural residues of AVOs detected in MDA-MB-231 cells, which were likewise increased upon PRIMA-1 treatment. Morphological evidence of the achievement of this final step may be considered the proof that in these cells treated with PRIMA-1, there is no block of autophagy completion.

Autophagy was induced by PRIMA-1 also in T1 cells lacking mutant p53, indicating that mutant p53 is not essential for the induction of autophagy upon PRIMA-1 exposure. However, these cells appeared to express a higher level of LC3 puncta already in the absence of treatment. Upon 200 μM PRIMA-1 the autophagic markers increased, although to a lower extent than in MDA-MB-231 cells. Indeed, the number of AVs in 200 μM PRIMA-1 treated compared to untreated cells increased 13-fold in MDA-MB-231 and and 5-fold in T1 cells. Likewise, the volume density of AVs increased up to 20-fold after PRIMA-1 in MDA-MB-231 but only up to 7-fold in T1 cells (Fig. 7). This suggests that the mutant p53 plays an inhibitory role on basal autophagy but its removal affects the regulation of autophagy, weakening its induction by PRIMA-1. These results are in keeping with the existence of a pro-survival function exerted by mutant p53 in these cells. As a matter of fact, compared to MDA-MB-231, T1 cells deprived of this function are more sensitive to PRIMA-1, although they maintain the same sensitivity to another type of molecule such as adriamycin [10].

The autophagic potential of PRIMA-1 has been detected also in HCT116 cancer cells, regardless the presence of wild type p53, again demonstrating that p53 is not essential for autophagy induction by this drug. However, in keeping with what has been already reported [26], our results show that wild type p53 can inhibit basal autophagy. Unlike what has been observed in T1, a significantly higher induction of autophagy was found in HCT116 p53 −/− than in HCT116 p53 +/+ cells upon 50 μM PRIMA-1 (Fig. 7), as if the absence of wild type p53 lowered the threshold for autophagy induction by PRIMA-1. Noteworthy, HCT116 p53 −/− cells were more sensitive to the cytotoxic effect of PRIMA-1 than HCT116 p53 +/+ cells (Fig. 4), suggesting that in these cells a deregulated autophagy may lead to cell death. It is to be noted that such a higher sensitivity of HCT116 p53 −/− cells towards PRIMA-1 is not a peculiarity of this cell line *per se*, since when other drugs, such as adriamycin or 5-fluorouracil, were used for survival experiments, HCT116 p53 −/− cells appeared even more viable than their p53 +/+ counterpart (data not shown). Although more experiments have to be performed on this issue, the greater sensitivity of cells lacking p53 towards PRIMA-1 combined with a deregulated autophagy may underline a role of autophagy in PRIMA-1 induced cell death. The link between autophagy and cell death is still a matter of discussion [43,44]. It has been reported that low levels of basal autophagy are pro-survival and help to maintain metabolic homeostasis. However, in some cellular settings or when it occurs to a remarkable extent, autophagy may contribute to or accompany cell death [42,45–47]. Interestingly, the apoptotic and the autophagic response machineries share common signals and a cross-talk between the two pathways indeed exists [19,45].

We have previously shown that in MDA-MB-231 cells treated with PRIMA-1, mutant p53 translocated into nucleoli in a high percentage of cells and this was associated to p53 degradation *via* ubiquitination, and cell death [10]. To our opinion, this could indicate the triggering of a protein degradation pathway that removes a pro-survival function of the mutant p53 [10]. Indeed, the degradation of mutant p53 induced by PRIMA-1 has been observed also in DLD1 cells (Supplementary Fig. 3). On the other hand, in HCT116 and MCF7 cells, the wild type p53 protein was induced (or stabilized) by treatment with PRIMA-1 (Supplementary Fig. 3). These results indicate that

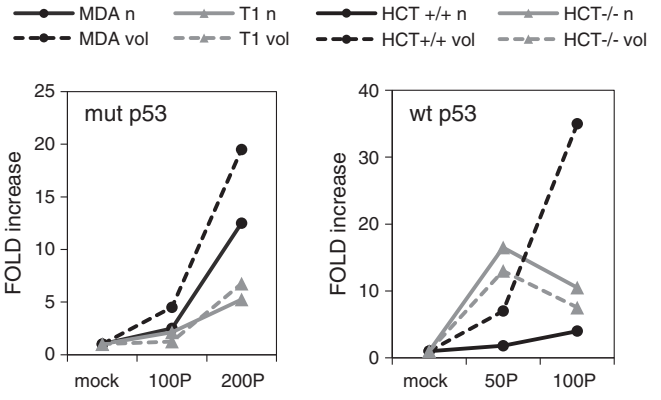

Fig. 7. Comparison of autophagy induction following PRIMA-1 in MDA-MB-231 (mut p53), HCT116 cells (wt p53) and their derivative p53 lacking cells. The fold increase of AV number (n) and volume density (vol) in treated *vs* untreated cells was calculated and reported for each cell line.

the autophagy observed after PRIMA-1 exposure is not a direct consequences of p53 induction, but again suggest a different role played by mutant and wild type p53 in cancer cells undergoing autophagy. In addition it should be mentioned that unfolded mutant p53 is preferentially modified by PRIMA-1/APR-246 as compared to the correctly folded wild type protein [3] implying that a different effect of PRIMA-1 directly on mutant or wild type p53 proteins is possible.

In conclusion, the data presented here showed for the first time that PRIMA-1 can trigger autophagy in cancer cells expressing both wild type and mutant p53. Furthermore, although autophagy was induced by PRIMA-1 regardless of the presence of p53, our results highlight a modulating role of p53 on autophagy triggered by this molecule. In particular, while wild type p53 may limit PRIMA-1 induced autophagy, mutant p53, likely due to a gain of function activity of this protein, may promote autophagy and sustain cell viability upon PRIMA-1. Since the methylated form of PRIMA-1, namely APR-246, is presently employed in phase I/II clinical trials for hematological malignancies and prostate cancer and a first-in-human study with this compound has been very recently published [41], these results could be of interest for its therapeutic use in cancer treatment.

Acknowledgements

This work was supported by a grant from the Associazione Italiana per la Ricerca sul Cancro (AIRC) to G. Fronza (IG#5506). G. Foggetti is on a PhD program of the School in Genetic Oncology and Developmental Biology, University of Genoa.

Appendix A. Supplementary data

Supplementary data to this article can be found online at http://dx.doi.org/10.1016/j.bbamcr.2013.03.020.

References

[1] G. Selivanova, K.G. Wiman, Reactivation of mutant p53: molecular mechanisms and therapeutic potential, Oncogene 26 (2007) 2243–2254.
[2] V.J. Bykov, N. Issaeva, G. Selivanova, K.G. Wiman, Mutant p53-dependent growth suppression distinguishes PRIMA-1 from known anticancer drugs: a statistical analysis of information in the National Cancer Institute database, Carcinogenesis 23 (2002) 2011–2018.
[3] J.M. Lambert, P. Gorzov, D.B. Veprintsev, M. Soderqvist, D. Segerback, J. Bergman, A.R. Fersht, P. Hainaut, K.G. Wiman, V.J. Bykov, PRIMA-1 reactivates mutant p53 by covalent binding to the core domain, Cancer Cell 15 (2009) 376–388.
[4] J.E. Chipuk, U. Maurer, D.R. Green, M. Schuler, Pharmacologic activation of p53 elicits Bax-dependent apoptosis in the absence of transcription, Cancer Cell 4 (2003) 371–381.
[5] J. Shen, H. Vakifahmetoglu, H. Stridh, B. Zhivotovsky, K.G. Wiman, PRIMA-1MET induces mitochondrial apoptosis through activation of caspase-2, Oncogene 27 (2008) 6571–6580.
[6] J.M. Lambert, A. Moshfegh, P. Hainaut, K.G. Wiman, V.J. Bykov, Mutant p53 reactivation by PRIMA-1(MET) induces multiple signaling pathways converging on apoptosis, Oncogene 29 (2009) 1329–1338.
[7] A.C. Koong, V. Chauhan, L. Romero-Ramirez, Targeting XBP-1 as a novel anti-cancer strategy, Cancer Biol. Ther. 5 (2006) 756–759.
[8] J. Li, B. Lee, A.S. Lee, Endoplasmic reticulum stress-induced apoptosis: multiple pathways and activation of p53-up-regulated modulator of apoptosis (PUMA) and NOXA by p53, J. Biol. Chem. 281 (2006) 7260–7270.
[9] N. Rokaeus, G. Klein, K.G. Wiman, L. Szekely, K. Mattsson, PRIMA-1(MET) induces nucleolar accumulation of mutant p53 and PML nuclear body-associated proteins, Oncogene 26 (2007) 982–992.
[10] D. Russo, L. Ottaggio, I. Penna, G. Foggetti, G. Fronza, A. Inga, P. Menichini, PRIMA-1 cytotoxicity correlates with nucleolar localization and degradation of mutant p53 in breast cancer cells, Biochem. Biophys. Res. Commun. 402 (2010) 345–350.
[11] S. He, J. Yaung, Y.H. Kim, E. Barron, S.J. Ryan, D.R. Hinton, Endoplasmic reticulum stress induced by oxidative stress in retinal pigment epithelial cells, Graefes Arch. Clin. Exp. Ophthalmol. 246 (2008) 677–683.
[12] C.X. Santos, L.Y. Tanaka, J. Wosniak, F.R. Laurindo, Mechanisms and implications of reactive oxygen species generation during the unfolded protein response: roles of endoplasmic reticulum oxidoreductases, mitochondrial electron transport, and NADPH oxidase, Antioxid. Redox Signal. 11 (2009) 2409–2427.
[13] S.A. Oakes, S.S. Lin, M.C. Bassik, The control of endoplasmic reticulum-initiated apoptosis by the BCL-2 family of proteins, Curr. Mol. Med. 6 (2006) 99–109.
[14] C.A. Hetz, ER stress signaling and the BCL-2 family of proteins: from adaptation to irreversible cellular damage, Antioxid. Redox Signal. 9 (2007) 2345–2355.
[15] H.M. Heath-Engel, N.C. Chang, G.C. Shore, The endoplasmic reticulum in apoptosis and autophagy: role of the BCL-2 protein family, Oncogene 27 (2008) 6419–6433.
[16] B. Levine, D.J. Klionsky, Development by self-digestion: molecular mechanisms and biological functions of autophagy, Dev. Cell 6 (2004) 463–477.
[17] N. Mizushima, Autophagy: process and function, Genes Dev. 21 (2007) 2861–2873.
[18] T. Shintani, D.J. Klionsky, Autophagy in health and disease: a double-edged sword, Science 306 (2004) 990–995.
[19] M.C. Maiuri, E. Zalckvar, A. Kimchi, G. Kroemer, Self-eating and self-killing: crosstalk between autophagy and apoptosis, Nat. Rev. Mol. Cell Biol. 8 (2007) 741–752.
[20] X.H. Liang, S. Jackson, M. Seaman, K. Brown, B. Kempkes, H. Hibshoosh, B. Levine, Induction of autophagy and inhibition of tumorigenesis by beclin 1, Nature 402 (1999) 672–676.
[21] C. Liang, P. Feng, B. Ku, I. Dotan, D. Canaani, B.H. Oh, J.U. Jung, Autophagic and tumour suppressor activity of a novel Beclin1-binding protein UVRAG, Nat. Cell Biol. 8 (2006) 688–699.
[22] B. Levine, Cell biology: autophagy and cancer, Nature 446 (2007) 745–747.
[23] Y. Kondo, T. Kanzawa, R. Sawaya, S. Kondo, The role of autophagy in cancer development and response to therapy, Nat. Rev. Cancer 5 (2005) 726–734.
[24] K.H. Vousden, D.P. Lane, P53 in health and disease, Nat. Rev. Mol. Cell Biol. 8 (2007) 275–283.
[25] M.C. Maiuri, L. Galluzzi, E. Morselli, O. Kepp, S.A. Malik, G. Kroemer, Autophagy regulation by p53, Curr. Opin. Cell Biol. 22 (2010) 181–185.
[26] E. Tasdemir, M.C. Maiuri, L. Galluzzi, I. Vitale, M. Djavaheri-Mergny, M. D'Amelio, A. Criollo, E. Morselli, C. Zhu, F. Harper, U. Nannmark, C. Samara, P. Pinton, J.M. Vicencio, R. Carnuccio, U.M. Moll, F. Madeo, P. Paterlini-Brechot, R. Rizzuto, G. Szabadkai, G. Pierron, K. Blomgren, N. Tavernarakis, P. Codogno, F. Cecconi, G. Kroemer, Regulation of autophagy by cytoplasmic p53, Nat. Cell Biol. 10 (2008) 676–687.
[27] D. Crighton, S. Wilkinson, J. O'Prey, N. Syed, P. Smith, P.R. Harrison, M. Gasco, O. Garrone, T. Crook, K.M. Ryan, DRAM, a p53-induced modulator of autophagy, is critical for apoptosis, Cell 126 (2006) 121–134.
[28] J. Bartek, R. Iggo, J. Gannon, D.P. Lane, Genetic and immunochemical analysis of mutant p53 in human breast cancer cell lines, Oncogene 5 (1990) 893–899.
[29] R. Magrini, D. Russo, L. Ottaggio, G. Fronza, A. Inga, P. Menichini, PRIMA-1 synergizes with adriamycin to induce cell death in non-small cell lung cancer cells, J. Cell. Biochem. 104 (2008) 2363–2373.
[30] R. Gallo, F. Gambelli, B. Gava, F. Sasdelli, V. Tellone, M. Masini, P. Marchetti, F. Dotta, V. Sorrentino, Generation and expansion of multipotent mesenchymal progenitor cells from cultured human pancreatic islets, Cell Death Differ. 14 (2007) 1860–1871.
[31] D.J. Klionsky, F.C. Abdalla, H. Abeliovich, R.T. Abraham, A. Acevedo-Arozena, K. Adeli, L. Agholme, M. Agnello, P. Agostinis, J.A. Aguirre-Ghiso, H.J. Ahn, O. Ait-Mohamed, S. Ait-Si-Ali, T. Akematsu, S. Akira, H.M. Al-Younes, M.A. Al-Zeer, M.L. Albert, R.L. Albin, J. Alegre-Abarrategui, M.F. Aleo, M. Alirezaei, A. Almasan, M. Almonte-Becerril, A. Amano, R. Amaravadi, S. Amarnath, A.O. Amer, N. Andrieu-Abadie, V. Anantharam, D.K. Ann, S. Anoopkumar-Dukie, H. Aoki, N. Apostolova, P. Auberger, M. Baba, S.K. Backues, E.H. Baehrecke, B.A. Bahr, X.Y. Bai, Y. Bailly, R. Baiocchi, G. Baldini, W. Balduini, A. Ballabio, B.A. Bamber, E.T. Bampton, G. Banhegyi, C.R. Bartholomew, D.C. Bassham, R.C. Bast Jr., H. Batoko, B.H. Bay, I. Beau, D.M. Bechet, T.J. Begley, C. Behl, C. Behrends, S. Bekri, B. Bellaire, L.J. Bendall, L. Benetti, L. Berliocchi, H. Bernardi, F. Bernassola, S. Besteiro, I. Bhatia-Kissova, X. Bi, M. Biard-Piechaczyk, J.S. Blum, L.H. Boise, P. Bonaldo, D.L. Boone, B.C. Bornhauser, K.R. Bortoluci, I. Bossis, F. Bost, J.P. Bourquin, P. Boya, M. Boyer-Guittaut, P.V. Bozhkov, N.R. Brady, C. Brancolini, A. Brech, J.E. Brenman, A. Brennand, E.H. Bresnick, P. Brest, D. Bridges, M.L. Bristol, P.S. Brookes, E.J. Brown, J.H. Brumell, N. Brunetti-Pierri, U.T. Brunk, D.E. Bulman, S.J. Bultman, G. Bultynck, L.F. Burbulla, W. Bursch, J.P. Butchar, W. Buzgariu, S.P. Bydlowski, K. Cadwell, M. Cahova, D. Cai, J. Cai, Q. Cai, B. Calabretta, J. Calvo-Garrido, N. Camougrand, M. Campanella, J. Campos-Salinas, E. Candi, L. Cao, A.B. Caplan, S.R. Carding, S.M. Cardoso, J.S. Carew, C.R. Carlin, V. Carmignac, L.A. Carneiro, S. Carra, R.A. Caruso, G. Casari, C. Casas, R. Castino, E. Cebollero, F. Cecconi, J. Celli, H. Chaachouay, H.J. Chae, C.Y. Chai, D.C. Chan, E.Y. Chan, R.C. Chang, C.M. Che, C.C. Chen, G.C. Chen, G.Q. Chen, M. Chen, Q. Chen, S.S. Chen, W. Chen, X. Chen, X. Chen, X. Chen, Y.G. Chen, Y. Chen, Y. Chen, Y.J. Chen, Z. Chen, A. Cheng, C.H. Cheng, Y. Cheng, H. Cheong, J.H. Cheong, S. Cherry, R. Chess-Williams, Z.H. Cheung, E. Chevet, H.L. Chiang, R. Chiarelli, T. Chiba, L.S. Chin, S.H. Chiou, F.V. Chisari, C.H. Cho, D.H. Cho, A.M. Choi, D. Choi, K.S. Choi, M.E. Choi, S. Chouaib, D. Choubey, V. Choubey, C.T. Chu, T.H. Chuang, S.H. Chueh, T. Chun, Y.J. Chwae, M.L. Chye, R. Ciarcia, M.R. Ciriolo, M.J. Clague, R.S. Clark, P.G. Clarke, R. Clarke, P. Codogno, H.A. Coller, M.I. Colombo, S. Comincini, M. Condello, F. Condorelli, M.R. Cookson, G.H. Coombs, I. Coppens, R. Corbalan, P. Cossart, P. Costelli, S. Costes, A. Coto-Montes, E. Couve, F.P. Coxon, J.M. Cregg, J.L. Crespo, M.J. Cronje, A.M. Cuervo, J.J. Cullen, M.J. Czaja, M. D'Amelio, A. Darfeuille-Michaud, L.M. Davids, F.E. Davies, M. De Felici, J.F. de Groot, C.A. de Haan, L. De Martino, A. De Milito, V. De Tata, J. Debnath, A. Degterev, B. Dehay, L.M. Delbridge, F. Demarchi, Y.Z. Deng, J. Dengjel, P. Dent, D. Denton, V. Deretic, S.D. Desai, R.J. Devenish, M. Di Gioacchino, G. Di Paolo, C. Di Pietro, G. Diaz-Araya, I. Diaz-Laviada, M.T. Diaz-Meco, J. Diaz-Nido, I. Dikic, S.P. Dinesh-Kumar, W.X. Ding, C.W. Distelhorst, A. Diwan, M. Djavaheri-Mergny, S. Dokudovskaya, Z. Dong, F.C. Dorsey, V. Dosenko, J.J. Dowling, S. Doxsey, M. Dreux, M.E. Drew, Q. Duan, M.A. Duchosal, K. Duff, I. Dugail, M. Durbeej, M. Duszenko, C.L. Edelstein, A.L. Edinger, G. Egea, L. Eichinger, N.T. Eissa, S. Ekmekcioglu, W.S. El-Deiry, Z. Elazar, M. Elgendy, L.M. Ellerby, K.E. Eng, A.M. Engelbrecht, S. Engelender, J. Erenpreisa, R. Escalante, A. Esclatine, E.L. Eskelinen, L. Espert, V. Espina, H. Fan, J. Fan, Q.W. Fan, Z. Fan, S. Fang, Y. Fang, M. Fanto, A. Fanzani, T. Farkas, J.C. Farre, M. Faure, M. Fechheimer, C.G. Feng, J. Feng, Q. Feng, Y. Feng, L. Fesus, R. Feuer, M.E. Figueiredo-Pereira, G.M. Fimia, D.C.

Fingar, S. Finkbeiner, T. Finkel, K.D. Finley, F. Fiorito, E.A. Fisher, P.B. Fisher, M. Flajolet, M.L. Florez-McClure, S. Florio, E.A. Fon, F. Fornai, F. Fortunato, R. Fotedar, D.H. Fowler, H.S. Fox, R. Franco, L.B. Frankel, M. Fransen, J.M. Fuentes, J. Fueyo, J. Fujii, K. Fujisaki, E. Fujita, M. Fukuda, R.H. Furukawa, M. Gaestel, P. Gailly, M. Gajewska, B. Galliot, V. Galy, S. Ganesh, B. Ganetzky, I.G. Ganley, F.B. Gao, G.F. Gao, J. Gao, L. Garcia, G. Garcia-Manero, M. Garcia-Marcos, M. Garmyn, A.L. Gartel, E. Gatti, M. Gautel, T.R. Gawriluk, M.E. Gegg, J. Geng, M. Germain, J.E. Gestwicki, D.A. Gewirtz, S. Ghavami, P. Ghosh, A.M. Giammarioli, A.N. Giatromanolaki, S.B. Gibson, R.W. Gilkerson, M.L. Ginger, E. Goncu, C. Gongora, C.D. Gonzalez, R. Gonzalez, C. Gonzalez-Estevez, R.A. Gonzalez-Polo, E. Gonzalez-Rey, N.V. Gorbunov, S. Gorski, S. Goruppi, R.A. Gottlieb, D. Gozuacik, G.E. Granato, G.D. Grant, K.N. Green, A. Gregorc, F. Gros, C. Grose, T.W. Grunt, P. Gual, J.L. Guan, K.L. Guan, S.M. Guichard, A.S. Gukovskaya, I. Gukovsky, J. Gunst, A.B. Gustafsson, A.J. Halayko, A.N. Hale, S.K. Halonen, M. Hamasaki, F. Han, T. Han, M.K. Hancock, M. Hansen, H. Harada, M. Harada, S.E. Hardt, J.W. Harper, A.L. Harris, J. Harris, S.D. Harris, M.J. Hebert, K.A. Heidenreich, M.H. Helfrich, G.V. Helgason, E.P. Henske, B. Herman, P.K. Herman, C. Hetz, S. Hilfiker, J.A. Hill, L.J. Hocking, P. Hofman, T.G. Hofmann, J. Hohfeld, T.L. Holyoake, M.H. Hong, D.A. Hood, G.S. Hotamisligil, E.J. Houwerzijl, M. Hoyer-Hansen, B. Hu, C.A. Hu, H.M. Hu, Y. Hua, C. Huang, J. Huang, S. Huang, W.P. Huang, T.B. Huber, W.K. Huh, T.H. Hung, T.R. Hupp, G.M. Hur, J.B. Hurley, S.N. Hussain, P.J. Hussey, J.J. Hwang, S. Hwang, A. Ichihara, S. Ilkhanizadeh, K. Inoki, T. Into, V. Iovane, J.L. Iovanna, N.Y. Ip, Y. Isaka, H. Ishida, C. Isidoro, K. Isobe, A. Iwasaki, M. Izquierdo, Y. Izumi, P.M. Jaakkola, M. Jaattela, G.R. Jackson, W.T. Jackson, B. Janji, M. Jendrach, J.H. Jeon, E.B. Jeung, H. Jiang, H. Jiang, J.X. Jiang, M. Jiang, Q. Jiang, X. Jiang, X. Jiang, A. Jimenez, M. Jin, S. Jin, C.O. Joe, T. Johansen, D.E. Johnson, G.V. Johnson, N.L. Jones, B. Joseph, S.K. Joseph, A.M. Joubert, G. Juhasz, L. Juillerat-Jeanneret, C.H. Jung, Y.K. Jung, K. Kaarniranta, A. Kaasik, T. Kabuta, M. Kadowaki, K. Kagedal, Y. Kamada, V.O. Kaminskyy, H.H. Kampinga, H. Kanamori, C. Kang, K.B. Kang, K.I. Kang, R. Kang, Y.A. Kang, T. Kanki, T.D. Kanneganti, H. Kanno, A.G. Kanthasamy, A. Kanthasamy, V. Karantza, G.P. Kaushal, S. Kaushik, Y. Kawazoe, P.Y. Ke, J.H. Kehrl, A. Kelekar, C. Kerkhoff, D.H. Kessel, H. Khalil, J.A. Kiel, A.A. Kiger, A. Kihara, D.R. Kim, D.H. Kim, D.H. Kim, E.K. Kim, H.R. Kim, J.S. Kim, J.H. Kim, J.C. Kim, J.K. Kim, P.K. Kim, S.W. Kim, Y.S. Kim, Y. Kim, A. Kimchi, A.C. Kimmelman, J.S. King, T.J. Kinsella, V. Kirkin, L.A. Kirshenbaum, K. Kitamoto, K. Kitazato, L. Klein, W.T. Klimecki, J. Klucken, E. Knecht, B.C. Ko, J.C. Koch, H. Koga, J.Y. Koh, Y.H. Koh, M. Koike, M. Komatsu, E. Kominami, H.J. Kong, W.J. Kong, V.I. Korolchuk, Y. Kotake, M.I. Koukourakis, J.B. Kouri Flores, A.L. Kovacs, C. Kraft, D. Krainc, H. Kramer, C. Kretz-Remy, A.M. Krichevsky, G. Kroemer, R. Kruger, O. Krut, N.T. Ktistakis, C.Y. Kuan, R. Kucharczyk, A. Kumar, R. Kumar, S. Kumar, M. Kundu, H.J. Kung, T. Kurz, H.J. Kwon, A.R. La Spada, F. Lafont, T. Lamark, J. Landry, J.D. Lane, P. Lapaquette, J.F. Laporte, L. Laszlo, S. Lavandero, J.N. Lavoie, R. Layfield, P.A. Lazo, W. Le, L. Le Cam, D.J. Ledbetter, A.J. Lee, B.W. Lee, G.M. Lee, J. Lee, J.H. Lee, M. Lee, M.S. Lee, S.H. Lee, C. Leeuwenburgh, P. Legembre, R. Legouis, M. Lehmann, H.Y. Lei, Q.Y. Lei, D.A. Leib, J. Leiro, J.J. Lemasters, A. Lemoine, M.S. Lesniak, D. Lev, V.V. Levenson, B. Levine, E. Levy, F. Li, J.L. Li, L. Li, S. Li, W. Li, X.J. Li, Y.B. Li, Y.P. Li, C. Liang, Q. Liang, Y.F. Liao, P.P. Liberski, A. Lieberman, H.J. Lim, K.L. Lim, K. Lim, C.F. Lin, F.C. Lin, J. Lin, J.D. Lin, K. Lin, W.W. Lin, W.C. Lin, Y.L. Lin, R. Linden, P. Lingor, J. Lippincott-Schwartz, M.P. Lisanti, P.B. Liton, B. Liu, C.F. Liu, K. Liu, L. Liu, Q.A. Liu, W. Liu, Y.C. Liu, Y. Liu, R.A. Lockshin, C.N. Lok, S. Lonial, B. Loos, G. Lopez-Berestein, C. Lopez-Otin, L. Lossi, M.T. Lotze, P. Low, B. Lu, B. Lu, Z. Lu, F. Luciano, N.W. Lukacs, A.H. Lund, M.A. Lynch-Day, Y. Ma, F. Macian, J.P. MacKeigan, K.F. Macleod, F. Madeo, L. Maiuri, M.C. Maiuri, D. Malagoli, M.C. Malicdan, W. Malorni, N. Man, E.M. Mandelkow, S. Manon, I. Manov, K. Mao, X. Mao, Z. Mao, P. Marambaud, D. Marazziti, Y.L. Marcel, K. Marchbank, P. Marchetti, S.J. Marciniak, M. Marcondes, M. Mardi, G. Marfe, G. Marino, M. Markaki, M.R. Marten, S.J. Martin, C. Martinand-Mari, W. Martinet, M. Martinez-Vicente, M. Masini, P. Matarrese, S. Matsuo, R. Matteoni, A. Mayer, N.M. Mazure, D.J. McConkey, M.J. McConnell, C. McDermott, C. McDonald, G.M. McInerney, S.L. McKenna, B. McLaughlin, P.J. McLean, C.R. McMaster, G.A. McQuibban, A.J. Meijer, M.H. Meisler, A. Melendez, T.J. Melia, G. Melino, M.A. Mena, J.A. Menendez, R.F. Menna-Barreto, M.B. Menon, F.M. Menzies, C.A. Mercer, A. Merighi, D.E. Merry, S. Meschini, C.G. Meyer, T.F. Meyer, C.Y. Miao, J.Y. Miao, P.A. Michels, C. Michiels, D. Mijaljica, A. Milojkovic, S. Minucci, C. Miracco, C.K. Miranti, I. Mitroulis, K. Miyazawa, N. Mizushima, B. Mograbi, S. Mohseni, X. Molero, B. Mollereau, F. Mollinedo, T. Momoi, I. Monastyrska, M.M. Monick, M.J. Monteiro, M.N. Moore, R. Mora, K. Moreau, P.I. Moreira, Y. Moriyasu, J. Moscat, S. Mostowy, J.C. Mottram, T. Motyl, C.E. Moussa, S. Muller, S. Muller, K. Munger, C. Munz, L.O. Murphy, M.E. Murphy, A. Musaro, I. Mysorekar, E. Nagata, K. Nagata, A. Nahimana, U. Nair, T. Nakagawa, K. Nakahira, H. Nakano, H. Nakatogawa, M. Nanjundan, N.I. Naqvi, D.P. Narendra, M. Narita, M. Navarro, S.T. Nawrocki, T.Y. Nazarko, A. Nemchenko, M.G. Netea, T.P. Neufeld, P.A. Ney, I.P. Nezis, H.P. Nguyen, D. Nie, I. Nishino, C. Nislow, R.A. Nixon, T. Noda, A.A. Noegel, A. Nogalska, S. Noguchi, L. Notterpek, I. Novak, T. Nozaki, N. Nukina, T. Nurnberger, B. Nyfeler, K. Obara, T.D. Oberley, S. Oddo, M. Ogawa, T. Ohashi, K. Okamoto, N.L. Oleinick, F.J. Oliver, L.J. Olsen, S. Olsson, O. Opota, T.F. Osborne, G.K. Ostrander, K. Otsu, J.H. Ou, M. Ouimet, M. Overholtzer, B. Ozpolat, P. Paganetti, U. Pagnini, N. Pallet, G.E. Palmer, C. Palumbo, T. Pan, T. Panaretakis, U.B. Pandey, Z. Papackova, I. Papassideri, I. Paris, J. Park, O.K. Park, J.B. Parys, K.R. Parzych, S. Patschan, C. Patterson, S. Pattingre, J.M. Pawelek, J. Peng, D.H. Perlmutter, I. Perrotta, G. Perry, S. Pervaiz, M. Peter, G.J. Peters, M. Petersen, G. Petrovski, J.M. Phang, M. Piacentini, P. Pierre, V. Pierrefite-Carle, G. Pierron, R. Pinkas-Kramarski, A. Piras, N. Piri, L.C. Platanias, S. Poggeler, M. Poirot, A. Poletti, C. Pous, M. Pozuelo-Rubio, M. Praetorius-Ibba, A. Prasad, M. Prescott, M. Priault, N. Produit-Zengaffinen, A. Progulske-Fox, T. Proikas-Cezanne, S. Przedborski, K. Przyklenk, R. Puertollano, J. Puyal, S.B. Qian, L. Qin, Z.H. Qin, S.E. Quaggin, N. Raben, H. Rabinowich, S.W. Rabkin, I. Rahman, A. Rami, G. Ramm, G. Randall, F. Randow, V.A. Rao, J.C. Rathmell, B. Ravikumar, S.K. Ray, B.H. Reed, J.C. Reed, F. Reggiori, A. Regnier-Vigoroux, A.S. Reichert, J.J. Reiners Jr., R.J. Reiter, J. Ren, J.L. Revuelta, C.J. Rhodes, K. Ritis, E. Rizzo, J. Robbins, M. Roberge, H. Roca, M.C. Roccheri, S. Rocchi, H.P. Rodemann, S. Rodriguez de Cordoba, B. Rohrer, I.B. Roninson, K. Rosen, M.M. Rost-Roszkowska, M. Rouis, K.M. Rouschop, F. Rovetta, B.P. Rubin, D.C. Rubinsztein, K. Ruckdeschel, E.B. Rucker III, A. Rudich, E. Rudolf, N. Ruiz-Opazo, R. Russo, T.E. Rusten, K.M. Ryan, S.W. Ryter, D.M. Sabatini, J. Sadoshima, T. Saha, T. Saitoh, H. Sakagami, Y. Sakai, G.H. Salekdeh, P. Salomoni, P.M. Salvaterra, G. Salvesen, R. Salvioli, A.M. Sanchez, J.A. Sanchez-Alcazar, R. Sanchez-Prieto, M. Sandri, U. Sankar, P. Sansanwal, L. Santambrogio, S. Saran, S. Sarkar, M. Sarwal, C. Sasakawa, A. Sasnauskiene, M. Sass, K. Sato, M. Sato, A.H. Schapira, M. Scharl, H.M. Schatzl, W. Scheper, S. Schiaffino, C. Schneider, M.E. Schneider, R. Schneider-Stock, P.V. Schoenlein, D.F. Schorderet, C. Schuller, G.K. Schwartz, L. Scorrano, L. Sealy, P.O. Seglen, J. Segura-Aguilar, I. Seiliez, O. Seleverstov, C. Sell, J.B. Seo, D. Separovic, V. Setaluri, T. Setoguchi, C. Settembre, J.J. Shacka, M. Shanmugam, I.M. Shapiro, E. Shaulian, R.J. Shaw, J.H. Shelhamer, H.M. Shen, W.C. Shen, Z.H. Sheng, Y. Shi, K. Shibuya, Y. Shidoji, J.J. Shieh, C.M. Shih, Y. Shimada, S. Shimizu, T. Shintani, O.S. Shirihai, G.C. Shore, A.A. Sibirny, S.B. Sidhu, B. Sikorska, E.C. Silva-Zacarin, A. Simmons, A.K. Simon, H.U. Simon, C. Simone, A. Simonsen, D.A. Sinclair, R. Singh, D. Sinha, F.A. Sinicrope, A. Sirko, P.M. Siu, E. Sivridis, V. Skop, V.P. Skulachev, R.S. Slack, S.S. Smaili, D.R. Smith, M.S. Soengas, T. Soldati, X. Song, A.K. Sood, T.W. Soong, F. Sotgia, S.A. Spector, C.D. Spies, W. Springer, S.M. Srinivasula, L. Stefanis, J.S. Steffan, R. Stendel, H. Stenmark, A. Stephanou, S.T. Stern, C. Sternberg, B. Stork, P. Stralfors, C.S. Subauste, X. Sui, D. Sulzer, J. Sun, S.Y. Sun, Z.J. Sun, J.J. Sung, K. Suzuki, T. Suzuki, M.S. Swanson, C. Swanton, S.T. Sweeney, L.K. Sy, G. Szabadkai, I. Tabas, H. Taegtmeyer, M. Tafani, K. Takacs-Vellai, Y. Takano, K. Takegawa, G. Takemura, F. Takeshita, N.J. Talbot, K.S. Tan, K. Tanaka, K. Tanaka, D. Tang, D. Tang, I. Tanida, B.A. Tannous, N. Tavernarakis, G.S. Taylor, G.A. Taylor, J.P. Taylor, L.S. Terada, A. Terman, G. Tettamanti, K. Thevissen, C.B. Thompson, A. Thorburn, M. Thumm, F. Tian, Y. Tian, G. Tocchini-Valentini, A.M. Tolkovsky, Y. Tomino, L. Tonges, S.A. Tooze, C. Tournier, J. Tower, R. Towns, V. Trajkovic, L.H. Travassos, T.F. Tsai, M.P. Tschan, T. Tsubata, A. Tsung, B. Turk, L.S. Turner, S.C. Tyagi, Y. Uchiyama, T. Ueno, M. Umekawa, R. Umemiya-Shirafuji, V.K. Unni, M.I. Vaccaro, E.M. Valente, G. Van den Berghe, I.J. van der Klei, W. van Doorn, L.F. van Dyk, M. van Egmond, L.A. van Grunsven, P. Vandenabeele, W.P. Vandenberghe, I. Vanhorebeek, E.C. Vaquero, G. Velasco, T. Vellai, J.M. Vicencio, R.D. Vierstra, M. Vila, C. Vindis, G. Viola, M.T. Viscomi, O.V. Voitsekhovskaja, C. von Haefen, M. Votruba, K. Wada, R. Wade-Martins, C.L. Walker, C.M. Walsh, J. Walter, X.B. Wan, A. Wang, C. Wang, D. Wang, F. Wang, F. Wang, G. Wang, H. Wang, H.G. Wang, H.D. Wang, J. Wang, K. Wang, M. Wang, R.C. Wang, X. Wang, X. Wang, Y.J. Wang, Y. Wang, Z. Wang, Z.C. Wang, Z. Wang, D.G. Wansink, D.M. Ward, H. Watada, S.L. Waters, P. Webster, L. Wei, C.C. Weihl, W.A. Weiss, S.M. Welford, L.P. Wen, C.A. Whitehouse, J.L. Whitton, A.J. Whitworth, T. Wileman, J.W. Wiley, S. Wilkinson, D. Willbold, R.L. Williams, P.R. Williamson, B.G. Wouters, C. Wu, D.C. Wu, W.K. Wu, A. Wyttenbach, R.J. Xavier, Z. Xi, P. Xia, G. Xiao, Z. Xie, Z. Xie, D.Z. Xu, J. Xu, L. Xu, X. Xu, A. Yamamoto, A. Yamamoto, S. Yamashina, M. Yamashita, X. Yan, M. Yanagida, D.S. Yang, E. Yang, J.M. Yang, S.Y. Yang, W. Yang, W.Y. Yang, Z. Yang, M.C. Yao, T.P. Yao, B. Yeganeh, W.L. Yen, J.J. Yin, X.M. Yin, O.J. Yoo, G. Yoon, S.Y. Yoon, T. Yorimitsu, Y. Yoshikawa, T. Yoshimori, K. Yoshimoto, H.J. You, R.J. Youle, A. Younes, L. Yu, L. Yu, S.W. Yu, W.H. Yu, Z.M. Yuan, Z. Yue, C.H. Yun, M. Yuzaki, O. Zabirnyk, E. Silva-Zacarin, D. Zacks, E. Zacksenhaus, N. Zaffaroni, Z. Zakeri, H.J. Zeh III, S.O. Zeitlin, H. Zhang, H.L. Zhang, J. Zhang, J.P. Zhang, L. Zhang, L. Zhang, M.Y. Zhang, X.D. Zhang, M. Zhao, Y.F. Zhao, Y. Zhao, Z.J. Zhao, X. Zheng, B. Zhivotovsky, Q. Zhong, C.Z. Zhou, C. Zhu, W.G. Zhu, X.F. Zhu, X. Zhu, Y. Zhu, T. Zoladek, W.X. Zong, A. Zorzano, J. Zschocke, B. Zuckerbraun, Guidelines for the use and interpretation of assays for monitoring autophagy, Autophagy 8 (2012) 445–544.

[32] E.R. Weibel, Stereological Methods, Academic Press, New York London, 1979.

[33] P. Marchetti, S. Del Guerra, L. Marselli, R. Lupi, M. Masini, M. Pollera, M. Bugliani, U. Boggi, F. Vistoli, F. Mosca, S. Del Prato, Pancreatic islets from type 2 diabetic patients have functional defects and increased apoptosis that are ameliorated by metformin, J. Clin. Endocrinol. Metab. 89 (2004) 5535–5541.

[34] Y.A. Abassi, B. Xi, W. Zhang, P. Ye, S.L. Kirstein, M.R. Gaylord, S.C. Feinstein, X. Wang, X. Xu, Kinetic cell-based morphological screening: prediction of mechanism of compound action and off-target effects, Chem. Biol. 16 (2009) 712–723.

[35] S. Paglin, T. Hollister, T. Delohery, N. Hackett, M. McMahill, E. Sphicas, D. Domingo, J. Yahalom, A novel response of cancer cells to radiation involves autophagy and formation of acidic vesicles, Cancer Res. 61 (2001) 439–444.

[36] T. Kanzawa, Y. Kondo, H. Ito, S. Kondo, I. Germano, Induction of autophagic cell death in malignant glioma cells by arsenic trioxide, Cancer Res. 63 (2003) 2103–2108.

[37] T. Kanzawa, I.M. Germano, T. Komata, H. Ito, Y. Kondo, S. Kondo, Role of autophagy in temozolomide-induced cytotoxicity for malignant glioma cells, Cell Death Differ. 11 (2004) 448–457.

[38] H. Takeuchi, Y. Kondo, K. Fujiwara, T. Kanzawa, H. Aoki, G.B. Mills, S. Kondo, Synergistic augmentation of rapamycin-induced autophagy in malignant glioma cells by phosphatidylinositol 3-kinase/protein kinase B inhibitors, Cancer Res. 65 (2005) 3336–3346.

[39] Y. Kabeya, N. Mizushima, T. Ueno, A. Yamamoto, T. Kirisako, T. Noda, E. Kominami, Y. Ohsumi, T. Yoshimori, LC3, a mammalian homologue of yeast Apg8p, is localized in autophagosome membranes after processing, EMBO J. 19 (2000) 5720–5728.

[40] I. Tanida, N. Minematsu-Ikeguchi, T. Ueno, E. Kominami, Lysosomal turnover, but not a cellular level, of endogenous LC3 is a marker for autophagy, Autophagy 1 (2005) 84–91.

[41] S. Lehmann, V.J. Bykov, D. Ali, O. Andren, H. Cherif, U. Tidefelt, B. Uggla, J. Yachnin, G. Juliusson, A. Moshfegh, C. Paul, K.G. Wiman, P.O. Andersson, Targeting p53 *in vivo*: a first-in-human study with p53-targeting compound APR-246 in refractory hematologic malignancies and prostate cancer, J. Clin. Oncol. 30 (2012) 3633–3639.

[42] C. He, D.J. Klionsky, Regulation mechanisms and signaling pathways of autophagy, Annu. Rev. Genet. 43 (2009) 67–93.

[43] E.H. Baehrecke, Autophagy: dual roles in life and death? Nat. Rev. Mol. Cell Biol. 6 (2005) 505–510.

[44] S. Shen, O. Kepp, G. Kroemer, The end of autophagic cell death? Autophagy 8 (2012) 1–3.
[45] A. Eisenberg-Lerner, S. Bialik, H.U. Simon, A. Kimchi, Life and death partners: apoptosis, autophagy and the cross-talk between them, Cell Death Differ. 16 (2009) 966–975.
[46] W.X. Ding, H.M. Ni, W. Gao, Y.F. Hou, M.A. Melan, X. Chen, D.B. Stolz, Z.M. Shao, X.M. Yin, Differential effects of endoplasmic reticulum stress-induced autophagy on cell survival, J. Biol. Chem. 282 (2007) 4702–4710.
[47] S. Orrenius, V.O. Kaminskyy, B. Zhivotovsky, Autophagy in toxicology: cause or consequence? Annu. Rev. Pharmacol. Toxicol. (2012).